SEMARAK ILMU PUBLISHING

CFD Letters

Journal homepage:
https://semarakilmu.com.my/journals/index.php/CFD_Letters/index
ISSN: 2180-1363

Magnetohydrodynamic Stagnation Point Flow and Heat Transfer of Casson Fluids over a Stretching Sheet

Srikantha Setty B[1], Mani Ramanuja[1], Gopi Krishna G[1], Hanumesh Vaidya[2], K V Prasad[2], Rajashekhar Choudhari[3], Ashwini Bhat[4,*], Nagaraj N Katagi[4]

[1] Department of Mathematics, Marri Laxman Reddy Institute of Technology &Management, Dundigal, Hyderabad – 500 043, India
[2] Department of Mathematics, Vijayanagara Sri Krishnadevaraya University, Ballari: 583105, Karnataka, India
[3] Department of Mathematics, Manipal Institute of Technology Bengaluru, Manipal Academy of Higher Education, Manipal, Karnataka, India
[4] Department of Mathematics, Manipal Institute of Technology, Manipal Academy of Higher Education, Manipal, India

ARTICLE INFO

Article history:
Received 19 February 2024
Received in revised form 20 March 2024
Accepted 21 April 2024
Available online 30 September 2024

Keywords:
Magnetohydrodynamics (MHD); Casson fluid; Thermal conductivity; Radiation; Optimal Homotopy Analysis Method (OHAM)

ABSTRACT

This research investigates the effects of heat transfer on the stagnation-point flow of a non-Newtonian Casson fluid in a two-dimensional magnetohydrodynamic (MHD) boundary layer over a stretched sheet, considering thermal radiation impacts. By employing similarity transformations, the governing partial differential equations are transformed into nonlinear ordinary differential equations. The obtained self-similar equations are numerically solved using the Optimal Homotopy Analysis Method (OHAM). The numerical results are graphically represented, showcasing the influence of various parameters on fluid flow and heat transfer characteristics. The study uncovers important dynamics in transport phenomena. Examining and illustrating the effects of dimensionless parameters on velocity, temperature, and concentration profiles reveal significant insights. Moreover, skin friction and Nusselt number results for Casson fluids are analyzed and presented. The findings indicate that the Casson parameter and Hartman number act in opposition to fluid momentum, while the thermal conductivity parameter enhances fluid temperature. Thus, this research provides valuable insights into MHD boundary layer flows of non-Newtonian Casson fluids with thermal radiation effects, and the OHAM solution method proves effective in predicting flow transport properties.

1. Introduction

Non-Newtonian fluid flow through different geometries has attracted extensive research interest in recent years due to the wide applications in industrial and engineering domains such as oil extraction, paper, detergent, and syrup production. Casson fluid is a non-Newtonian fluid with distinct characteristics, behaving like an elastic solid and exhibiting yield stress in its constitutive relation. Unlike traditional Newtonian fluids, they exhibit a yield stress, indicating that they require a certain threshold of applied force to initiate flow. This characteristic sets them apart from Newtonian fluids, where viscosity remains constant regardless of shear rate. However, what

* *Corresponding author.*
E-mail address: ashwini.bhat@manipal.edu (Ashwini Bhat)

https://doi.org/10.37934/cfdl.17.2.163178

distinguishes Casson fluids is their unique response to shear, characterized by a sudden jump from zero shear stress to a finite value at the yield point. This behaviour contrasts with other non-Newtonian models, where the shear stress gradually increases with an increasing shear rate. Additionally, the Casson model captures shear-thinning behavior, where the apparent viscosity decreases with increasing shear rate, a feature crucial in understanding various practical applications ranging from biomedical to industrial processes. Casson fluid transport phenomena occur across various mechanical, chemical, and food processing engineering branches. Various materials, including blood, mud, emulsions, paints, sugar solutions, and tomato pastes, exhibit non-Newtonian properties and are pertinent to these applications. Heat transfer fluids like mineral oils and ethylene glycol also have critical industrial applications in power generation, air conditioning, microelectronics, etc. However, their performance is constrained by low thermal conductivities, limiting usage in heat exchangers. Consequently, substantial research in the past decade has focused on Casson fluids with enhanced thermal conductivity and variable viscosity. Understanding conductivity is vital as it governs heat transfer between the fluid and the surface.

The investigation into non-Newtonian fluids, particularly the Casson fluid [1], unveils a distinctive yield stress phenomenon. This fluid model applies to various substances like chocolate, honey, and blood. Notably, silicon suspensions, toners in water, and lithographic varnishes in printing inks exhibit nonlinear interactions between stress and strain velocity, as explained by the Casson fluid constitutive equation. Fredrickson [2] analyzed steady flow in a pipe for Casson fluid, and Attia [3] explored the impact of temperature-dependent thermal conductivity and viscosity. The study established that an increase in the variable viscosity parameter enhances fluid flow and heat transfer while variable thermal conductivity diminishes both. Mitsoulis [4] further delved into various benchmark problems related to viscoplastic flows. Kameswaran *et al.,* [5] investigated the two-dimensional boundary-layer flow of Newtonian fluid due to a stretching sheet saturated in nanofluid with chemical reactions. Hayat *et al.,* [6] focused on Soret and Dufour's effects in the magnetohydrodynamic (MHD) flow of Casson fluid. Jawali *et al.,* [7] explored the combined influence of thermal conductivity and variable viscosity on free convection fluid flow in a vertical channel.

A comprehensive exploration of slip, chemical reactions, and electrically conducting fluid above a nonlinearly permeable stretching sheet was conducted by Yazdi *et al.,* [8]. Bhattacharyya and Layek [9] studied the impact of velocity slip on viscous fluid's boundary layer fluid flow past a permeable stretching sheet in the presence of chemical reactions. Yasir Khan *et al.,* [10] analyzed the effects of variable liquid properties on a thin film over a stretching/shrinking sheet using the homotopy method. Mukhopadhyay [11] emphasized that understanding fluid dynamics and heat transfer relies heavily on comprehending the flow field of non-Newtonian fluids in a boundary layer adjacent to a stretching sheet. Afif [12] delved into the response of Casson nanofluid to chemical reactions and viscous dissipation. Aurangzaib *et al.,* [13] theoretically explored the pressure of heat radiation on irregular natural convection flow induced by stretching surfaces in the presence of a chemical reaction and a magnetic field. Shehzad *et al.,* [14] described the magnetic field's effect on Casson fluid mass-transfer flow via a permeable stretched sheet with a concurrent chemical reaction. Pal and Mandal [15] discussed the properties of mixed nanofluid convection flow on a stretching sheet, considering thermal radiation and chemical reactions. Similar solutions were obtained for the Casson fluid's unstable boundary flow caused by a stretching sheet immersed in a porous medium with first-order chemical processes.

Gireesha *et al.,* [16] focused on the magnetohydrodynamic (MHD) movement of a Casson-nanofluid past a nonlinearly stretched sheet, considering nonlinear radioactive heat transfer. Arshad *et al.,* [17] studied the MHD movement of sodium alginate-based Casson nanofluid across a porous medium with Newtonian heating. Ibrahim *et al.,* [18] investigated the similarity between solutions

for Casson nanofluid flow over a vertically exponentially stretched cylinder. Animasaun [19] presented non-draconian magnetohydrodynamic dissipative dynamics for Casson fluid flows over a linearly stretched surface, considering the impact of various thermophysical parameters. Damseh *et al.,* [20], Magyar and Chamkha [21], and Malik *et al.,* [22] explored the steady-state boundary layer flow of micropolar fluid induced by nonlinearly stretching sheets. Pramanik [23] studied the thermal radiation impact on Casson fluid past an exponentially permeable stretching surface, while Siddiqui *et al.,* [24] investigated two-dimensional MHD compress flow between similar plates. Prasad *et al.,* [25, 26] found that Casson nanofluid flow over a variable thickness stretching sheet/disk decelerates with suction and provides conflicting results with injection. The effect of chemical reactions and variable liquid properties on Casson fluid over a rotational disk in the presence of variable thickness was investigated by Vaidya *et al.,* [27, 28]. Ramanuja *et al.,* [29, 30] discussed the radiation effects of Newtonian/non-Newtonian fluids through porous medium.

Dharmendar *et al.,* [31] investigated magnetohydrodynamic, dissipative, and mixed convection boundary layer copper-water nanofluid fluid flow over a nonlinear stretching/shrinking sheet in the existence of heat generation/absorption and viscous dissipation. Goud *et al.,* [32] investigate the mass and heat transport phenomena associated with micropolar fluid flow created by a vertically stretched Riga surface. A numerical study of chemically reactive effects on magnetohydrodynamics (MHD) free convective unsteady flowing over an inclined plate in a porous material viscous dissipation was examined by Bejawada *et al.,* [33]. Wuriti *et al.,* [34] explored the impact of the Soret and Dufour properties, as well as the radiative phenomena, was noticed. The assumed flow was due to the stretched cylinder. Shankar *et al.,* [35] explored the characterization of the flow phenomena of hydromagnetic nanofluid thermal stratified through the porous medium due to the influence of the radiative heat energy.

Mahmood *et al.,* [36] examined the laminar and incompressible MHD oblique stagnation point flow of nanofluids over a stretched convective surface. Khadija *et al.,* [37] explored the primary goal of this research, which was to find out how nonlinear radiation, changes in viscosity, and aggregation affect the flow of ethylene glycol-based nanofluids in three dimensions. Adnan *et al.,* [38] examined the transformation of shape-memory alloys to high-temperature shape-memory alloys, which could be achieved by adding alloying elements or heat treatment. Bilal *et al.,* [39] reported the mass and energy transmission characteristics of an electrically conducting mixed convective nanofluid flow past a stretching Riga plate. Khadija *et al.,* [40] explored the industrial sector, which showed a growing interest in hybrid nanofluids affected by magnetohydrodynamics (MHD) owing to their wide range of applications, including photovoltaic water heaters and scraped surface heat exchangers.

Motivated by the above reference work and the numerous possible industrial applications, viz., polymer processing, coating and printing process, biomedical arena (blood flow modeling), and heat exchangers or fluid flow systems of power generation units, it is of paramount interest in this study to investigate the MHD stagnation point flow and heat transfer of Casson fluids over a stretching sheet. To analyze these complex fluid dynamics scenarios, the governing nonlinear partial differential equations (PDEs) are reduced to non-dimensional ordinary differential equations (ODEs) using similarity transformations. The "Optimal Homotopy Analysis Method (OHAM)" is employed to solve the transformed nonlinear coupled ODEs numerically.

2. Mathematical Modeling

Steady, 2-dimensional, viscous, and electrically non-Newtonian Casson fluid over a stretching sheet with variable thickness in the presence of variable viscosity and variable thermal conductivity is considered, the observable design depicted in Figure 1.

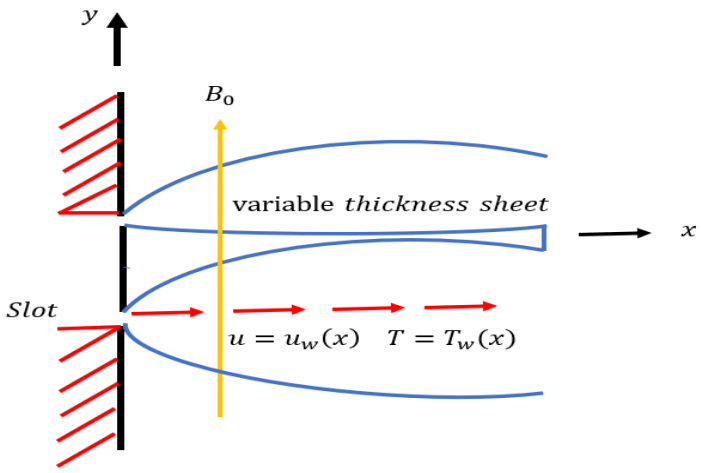

Fig. 1. Physical model

The rheological Equation of state for an isotropic and incompressible stagnation-point flow of a Casson fluid is considered. The fluid properties, including viscosity, consistency index, and thermal conductivity, are assumed to be uniform. Heat source and chemical reaction effects are also incorporated into the flow analysis. The Casson fluid satisfies the following rheological Equation of state for isotropic and incompressible conditions:

$$\tau_{ij} = \begin{cases} 2(\mu_B + \frac{p_y}{\sqrt{2\pi}})\mathrm{e}_{ij} & \pi > \pi_c \\ 2(\mu_B + \frac{p_y}{\sqrt{2\pi_c}})\mathrm{e}_{ij} & \pi < \pi_c \end{cases}$$

Where, π = $e_{ij}e_{ij}$ = product of the deformation rate with fluid consistency coefficient, $p_y = \frac{\mu_B\sqrt{2\pi}}{\beta}$ = yield stress, $e_{ij}e_{ij} = \frac{1}{2}\left(\frac{\partial u_i}{\partial x_j} + \frac{\partial u_j}{\partial x_i}\right)$ = Rate of strain tenor, e_{ij} is the $(i,j)\mathrm{th}$ component of deformation rate, n is the product of deformation rate with itself, π_c is a critical value of this product based on the non-Newtonian model, β Casson parameter, $\mu_B + \frac{P_Y}{\sqrt{2\pi}}$ is the plastic dynamic viscosity (μ_f) of the non-Newtonian fluid. The steady two-dimensional MHD flow of an electrically conducting non-Newtonian Casson fluid over a stretching sheet placed at $y = 0$. The flow is restricted in the region $y > 0$. The wall is stretched while the origin is stationary as the equal and opposite forces are applied along the x-axis. Consider a thin elastic sheet that emerges from a narrow slit at the origin of a Cartesian co-odorant System. The continuous sheet at $y = 0$ moves in its own plate with velocity: Yasir Khan *et al.,* [10]

$$U = bx \tag{1}$$

Where $b < 0$ corresponding to the shrinking and $b > 0$ corresponding to stretching and the surface temperature T_s is defined as

$$T_s = T_{ref}\left[\frac{bx^2}{2v_0}\right] + T_0 \tag{2}$$

Where T_{ref} taken as constant reference temperature, T_0 is the temperature at the slit and such that $0 \le T_{ref} \le T_0$. The variation of the thermal conductivity with temperature and viscosity of the fluid is assumed to be in the form given below.

$$k(\mathrm{T}) = k_0\left[1 + c(T - T_0)\right] \tag{3}$$

$$\mu(T) = \mu_0 e^{-\xi(\mathrm{T}-\mathrm{T}_0)} \tag{4}$$

Where k_0 and μ_0 be the viscosity and conductivity of the fluid, respectively at slit temperature T_0. The velocity and temperature field in the thin fluid layer is governed by the two-dimensional layer equations for continuity, momentum, and energy, which are included in the flow. (Yasir Khan *et al.,* [10])

$$\frac{\partial u}{\partial x} + \frac{\partial v}{\partial y} = 0 \tag{5}$$

$$u\frac{\partial u}{\partial x} + v\frac{\partial u}{\partial y} = \frac{1}{\rho_0}\left(1 + \frac{1}{\beta}\right)\frac{\partial}{\partial y}\left(\mu(T)\frac{\partial u}{\partial y}\right) - \frac{\sigma B_0^2 u}{\rho_0} \tag{6}$$

$$u\frac{\partial T}{\partial x} + v\frac{\partial T}{\partial y} = \frac{1}{\rho_{0C_P}}\frac{\partial}{\partial y}\left(\mathrm{k}(T)\frac{\partial T}{\partial y}\right) - \frac{1}{\rho_{0C_P}}\frac{\partial q_r}{\partial y} \tag{7}$$

Where u and v are the velocity components along x-and y-direction respectively, $\mu(T)$ is the variable viscosity, $k(T)$ is the variable thermal conductivity, c_p being specific heat, ρ_0 is the density of the fluid, B_0 is the magnetic field parameter, σ_0 defines fluid electrical conductivity, q_r being the radioactive heat-flux. The conditions that determine the behavior of a system at its boundary situation are given by,

$$\begin{aligned} &u = U; \quad v = -V_0 && T = T_0 \quad at \;\; y = 0 \\ &\mu\frac{\partial u}{\partial y} = \frac{\partial T}{\partial y} = 0 && v = u\frac{du}{dx} \quad at \; y = h \end{aligned} \tag{8}$$

Where V_0 be the suction velocity, h be the thickness of the film, μ be the viscosity of the fluid.

The radiation heat flux q_r is modeled by using Rossel and approximation (Brewster [41]); the radiative heat flux q_r is given by,

$$q_r = -\left(\frac{4\sigma^*}{3k}\right)\frac{\partial T'^4}{\partial y} \tag{9}$$

Where k is the coefficient of absorption, $\sigma*$ is the Stefan-Boltzmann constant. It is also assumed that if the temperature with in flow is T^4, then T^4 can be expressed as a linear combination of the temperature, then expansion of T^4 by using Taylors series method about T_H is obtained as$T^4 = T^4 + 4T^3(T - T_H) + 6T_H(T - T_H)^2 + \cdots$, neglecting second the higher-order terms, leads to $\mathrm{T}^4 \equiv 4T_H^3 T - 3T_H^4$

So that,

$$\frac{\partial q_r}{\partial y} = \frac{-16\sigma^* T_H^3}{3k^*}\frac{\partial^2 T}{\partial y^2} \tag{10}$$

Using Eq. (7) and Eq. (10) can be written as

$$u\frac{\partial T}{\partial x} + v\frac{\partial T}{\partial y} = \frac{1}{\rho_{0C_P}}\frac{\partial}{\partial y}\left(\mathrm{k}(T)\frac{\partial T}{\partial y}\right) + \frac{1}{\rho_{0C_P}}\left(\frac{16\sigma^* T_H^3}{3k^*}\frac{\partial^2 T}{\partial y^2}\right) \tag{11}$$

By introducing the dimensionless variable $f(\eta)$ and $\theta(\eta)$ as,

$$\psi = (\mathrm{b}\nu)^{1/2} x f(\eta) \tag{12}$$

$$\eta = \left(\frac{bx^2}{v_0}\right)^{1/2} y \tag{13}$$

$$T = T_{ref} + \left(\frac{bx^2}{2v_0}\right)\theta(\eta) + T_0 \tag{14}$$

Where $\theta(\eta) = \dfrac{T - T_0}{T_S - T_0}$

Introducing the stream function, the continuity Eq. (2) is satisfied by introducing the stream function $\psi(x, \mathrm{y})$ such that,

$$u = \frac{\partial \psi}{\partial y} = bxf'(\eta); \quad v = -\frac{\partial \psi}{\partial x} = -\left(bv_0\right)^{1/2} f(\eta) \tag{15}$$

The mathematical problem defined in Eq. (6) to Eq. (15) are then transformed into a set of ordinary differential equations given by,

$$\left(1 + \frac{1}{\beta}\right)\left(f''' - A\theta' f'' - A\theta f''' + A^2\theta'\theta f''\right) + ff'' - f'^2 - Mnf' = 0 \tag{16}$$

$$\left(1 + \frac{4}{3}Rd\right)\theta'' - \delta\theta\theta'' + \mathrm{Pr}\, f\theta' - 2\,\mathrm{Pr}\, f'\theta - \delta\theta'^2 = 0 \tag{17}$$

With the transformed boundary conditions,

$$\begin{aligned} &f(0)=S, \quad f'(0)=-1, \quad f(\alpha)=0, \ f''(\alpha)=0 \\ &\theta(0)=1, \quad \theta'(\alpha)=1 \end{aligned} \tag{18}$$

Where

$$\delta=-C\left(T_S-T_0\right),\ \mathrm{Mn}=\frac{\sigma B_0^2}{\rho_0 b},\ A=-\zeta\left(T_S-T_0\right), S=\left(\frac{b v_0}{V_0^2}\right),$$

$$\Gamma=\left(\frac{b}{v_0}\right)^{1/2} h\ , \mathrm{Pr}=\frac{\mu_0 c_p}{k_0}, Rd=\frac{4\sigma^* T_H^3}{k^* k_0}$$

The expressions for local skin friction and local Nusselt number are derived as follows:

$$C_f=\left(1+\frac{1}{\beta}\right)\left(\frac{\left(\tau_{zr}\right)}{\rho_0\left(bx\right)^2}\right), \qquad Nu=\frac{x q_w}{k_0\left(T_S-T_0\right)}$$

3. Optimal Homotopy Analysis Method: (OHAM)

The governing equations comprise coupled nonlinear differential equations with variable fluid properties. The Optimal Homotopy Analysis Method (OHAM) is utilized to obtain analytical solutions to these Eq. (16) - Eq. (17) subject to the boundary conditions Eq. (18). OHAM divides nonlinear terms into infinite linear sub-problems, which are solved recursively.

In this technique, we have an advantage in selecting the linear operator and introducing initial approximation (Liao [42]). The initial guess for dimensionless velocity and temperature is given as,

$$f_0(\xi)=S-\eta+\left(\eta^2\left(\frac{\eta}{\beta}-3\right)\right)\left(\frac{S}{2\beta^2}-\frac{1}{2\beta}\right), \qquad \theta_0(\xi)=\frac{\eta^2}{2}-\beta\eta+1 \tag{19}$$

We choose the auxiliary linear operators in the form,

$$L_f=\frac{d^4}{d\eta^4}, \qquad L_\theta=\frac{d^2}{d\eta^2} \tag{20}$$

The expressions of exact residual error areas are as follows:

$$\bar{E}_p^f\left(\hbar_f\right)=\int_0^1\left(N_f\left[\sum_{j=0}^{p}\hat{f}_j(\eta)\right]\right)^2 d\eta, \quad \bar{E}_p^\theta\left(\hbar_\theta\right)=\int_0^1\left(N_\theta\left[\sum_{j=0}^{p}\hat{\theta}_j(\eta)\right]\right)^2 d\eta. \tag{21}$$

In spite of using exact residual errors, we used the average residual errors $\bar{E}_p^f\left(\hbar_f\right)$ and $\bar{E}_p^\theta\left(\hbar_\theta\right)$ because they take longer.

$$\bar{E}_p^f\left(\hbar_f\right)=\frac{1}{P+1}\sum_{j=0}^{P}\left(N_f\left[\hat{f}_{[P]}\left(\eta_j\right),\hat{\theta}_{[P]}\left(\eta_j\right)\right]\right)^2$$

$$\bar{E}_p^\theta\left(\hbar_\theta\right)=\frac{1}{P+1}\sum_{j=0}^{P}\left(N_\theta\left[\hat{\theta}_{[P]}\left(\eta_j\right),\hat{f}_{[P]}\left(\eta_j\right)\right]\right)^2.$$

$$\bar{E}_p^t\left(\hbar\right)=\bar{E}_p^f\left(\hbar_f\right)+\bar{E}_p^\theta\left(\hbar_\theta\right).$$

Where $\bar{E}_p^t\left(\hbar\right)$ is the total residual error, $\eta_j=j/P,\ j=0,1,..P.$ Now we minimize the error function $\bar{E}_p^f\left(\hbar_f\right)$ and $\bar{E}_p^\theta\left(\hbar_\theta\right)$ in $\hbar_f,\hbar_\theta$ and obtain the optimal value of $\hbar_f,\hbar_\theta$ for p[th] order approximation.

3.1 Validation of the Methodology

In the absence of Casson fluid, magnetic parameter and radiation parameter, i.e $\left(\frac{1}{\beta}\to 0, B_0\to 0, q_r\to 0\right)$, Eq. (6) and Eq. (11) become,

$$u\frac{\partial u}{\partial x}+v\frac{\partial u}{\partial y}=\frac{1}{\rho_0}\frac{\partial}{\partial y}\left(\mu(T)\frac{\partial u}{\partial y}\right) \tag{22}$$

$$u\frac{\partial T}{\partial x}+v\frac{\partial T}{\partial y}=\frac{1}{\rho_{0C_p}}\frac{\partial}{\partial y}\left(\mathrm{k}(T)\frac{\partial T}{\partial y}\right) \tag{23}$$

Using Eq. (12) – Eq. (15), the above equations reduce to following the form (Yasir Khan *et al.,* [10]).

$$f'''-A\theta' f''-A\theta f'''+A^2\theta'\theta f''+ff''-f'^2=0$$

$$\theta''-\delta\theta\theta''+\mathrm{Pr}\ f\theta'-2\,\mathrm{Pr}\ f'\theta-\delta\theta'^2=0$$

To validate the current technique, the obtained results are compared with those of Yasir Khan *et al.,* [10], and the comparison is discussed in Table 1. It is noted that an increase in the variable viscosity parameter leads to a decrease in skin friction. The exact pattern is observed in the absence of Casson fluid, magnetic parameter, and radiation parameter.

Table 1

Comparison results for skin friction coefficient when Pr=0.72, S=0.1

	Yasir Khan *et al.,* [10]	Present
A	$\left(\frac{1}{\beta}\to 0, B_0\to 0, q_r\to 0\right)$	$\left(\frac{1}{\beta}\to 0.1,\ Mn\to 0.5, q_r\to 0.1\right)$
	$f''(0)$	$f''(0)$
0.1	0.00972	0.00487
0.5	0.00955	0.00476
1	0.00924	0.00463

4. Results and Discussions

The numerical technique described above is applied across a range of values for various physical parameters. Specifically, the investigation considers different values for thermal radiation and the Prandtl number, with the exclusion of the Casson fluid parameter, magnetic parameter, thermal conductivity parameter, steadiness parameter, and temperature. The resulting transformed nonlinear coupled ordinary differential equations (ODEs) are then subjected to the numerical solution using the "Optimal Homotopy Analysis Method (OHAM)." It offers a robust approach to solving nonlinear ordinary differential equations arising from the similarity transformations applied to the governing partial differential equations. The convergence of OHAM solutions is ensured through iterative procedures. The method involves expanding the solution in a series form with unknown coefficients and then determining these coefficients by imposing boundary conditions or initial conditions. Convergence criteria are established to monitor the convergence of the series solution. Typically, the convergence of the series solution is assessed by comparing successive terms in the series and checking for convergence to a desired level of accuracy. Convergence of solutions is ensured by maintaining a stringent accuracy criterion of 6 decimal places. The convergence rate of the OHAM solutions typically exhibits exponential behavior, ensuring rapid convergence to the desired accuracy level.

In this study, the default values assigned to the various parameters are as β =1 to 10, A =0.1 Mn =0.1 to 0.5, Rd =0.1 to 0.7, $\Pr$ =0.72, δ =0.3 to 0.7, and S =0.1 to 0.3. These parameter values are systematically explored to analyze their influence on the system dynamics, and the OHAM method is applied for numerical solutions in this comprehensive parameter space.

In this section, the influence of various physical variables on velocity and temperature is visually interpreted through graphical representations. The key observations from the figures are summarized as follows. Examining Figure 2, the effect of the Casson parameter (β) on the velocity profile, it is apparent that as β approaches higher values, the fluid behaves more like a Newtonian fluid. Physically, an increase in β (as β→∞) leads to a decrease in yield stress, resulting in a noticeable reduction in velocity profiles, leading to a smoother transition between the fluid's behavior under different shear rates. Consequently, the velocity profile becomes more uniform and resembles that of a Newtonian fluid, which does not exhibit a yield stress. The impact of the variable viscosity parameter (A) on the momentum boundary layer thickness is illustrated in Figure 3. Increasing A brings about a decrease in the thickness of the momentum boundary layer. This phenomenon stems from the fact that larger values of A signify a greater temperature differential between the surface and the surrounding fluid. Consequently, the increased temperature gradient accelerates the fluid near the surface, thereby thinning the momentum boundary layer. Figure 4 shows the influence of the magnetic parameter (*Mn*) on the velocity profile $f'(\eta)$. A higher value of *Mn* opposes the fluid flow, attributed to the amplified Lorentz force generated by the larger *Mn* value, introducing resistance between particles and leading to a decrement in the velocity profile. The effect of the radiation parameter (Rd) on the temperature profile is depicted in Figure 5. An increase in Rd results in a significant decrement in the temperature profile. This is because of the mean absorption coefficient, which plays a vital role in decreasing the pattern. Figure 6 highlights the impact of the Prandtl number (*Pr*) on fluid temperature. Increasing *Pr* values enhance the fluid temperature; physically, the connection between the Casson fluid's kinematic viscosity and thermal diffusivity showcases a similar trend as observed in the case of the thermal conductivity parameter (δ) on the temperature $\theta(\eta)$ in Figure 7. Figure 8 illustrates the effect of the steadiness parameter (*S*) on the velocity profile. Increasing values of *S* cause resistance between fluid particles, leading to a decrease

in velocity profiles. These graphical interpretations provide valuable insights into how changes in each parameter affect the velocity and temperature profiles in the system.

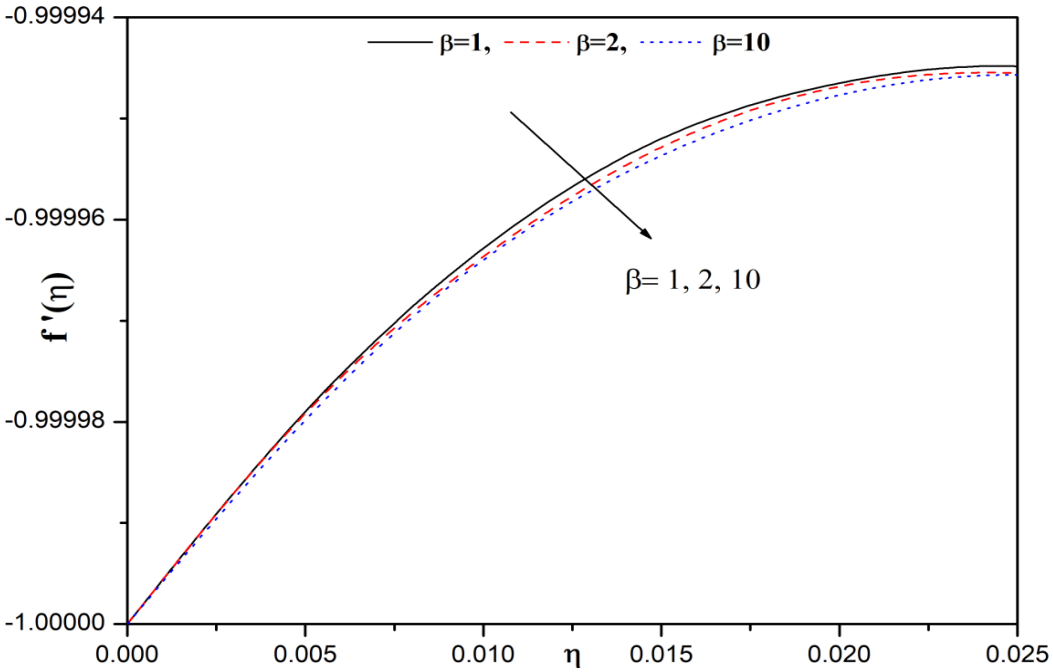

Fig. 2. Velocity profile for difference values of β with Pr=0.72, A=S= δ=Rd=α=0.1, Mn=0.5

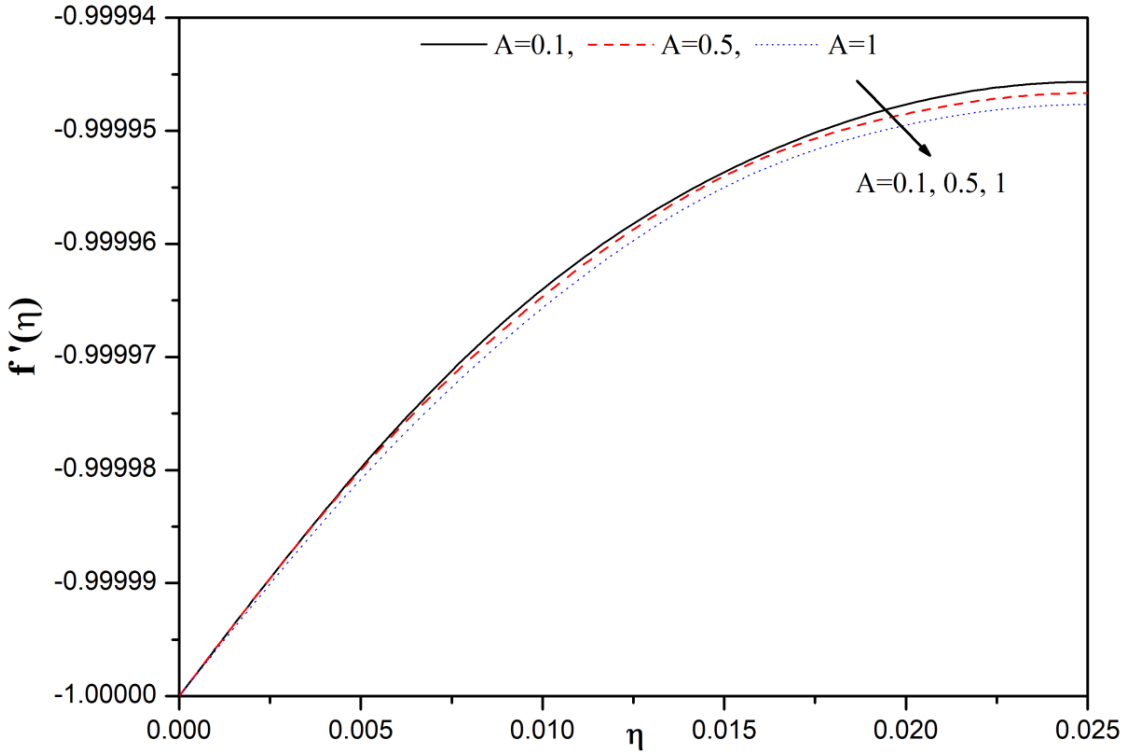

Fig. 3. Velocity profile for difference values of A with Pr=0.72, S= δ=Rd=α=0.1, β=10, Mn=0.5

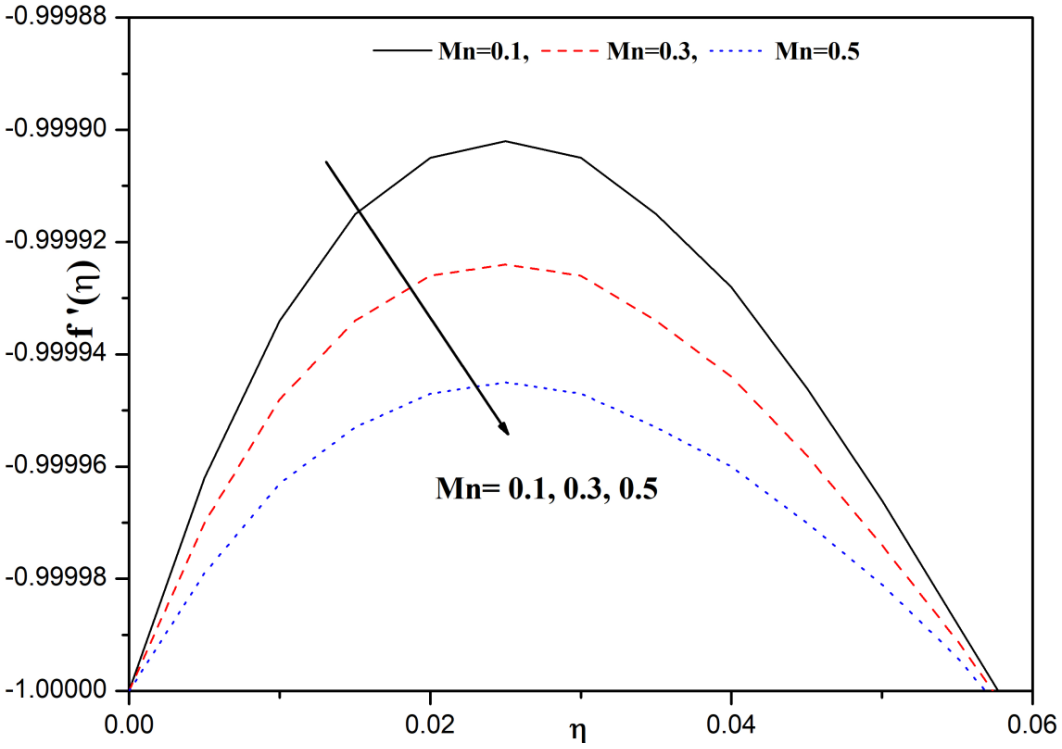

Fig. 4. Velocity profile for difference values of Mn with Pr=0.72, A=S= δ=Rd=α=0.1, β =10

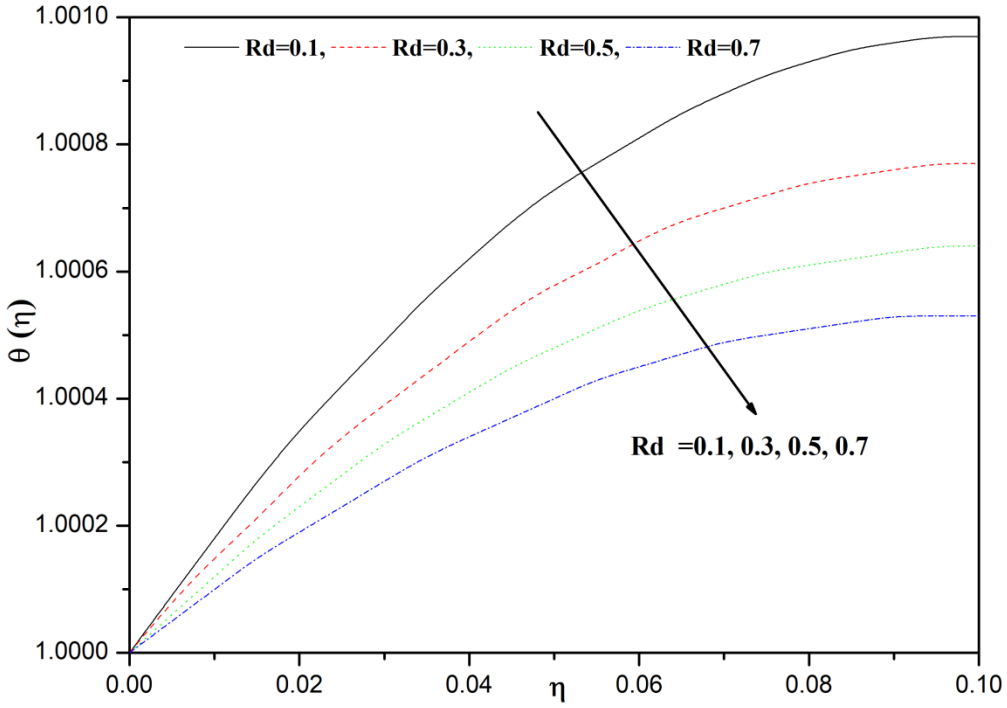

Fig. 5. Temperature profile for difference values of Rd with Pr=0.72, S= δ=A=α=0.1, β =10, Mn=0.5

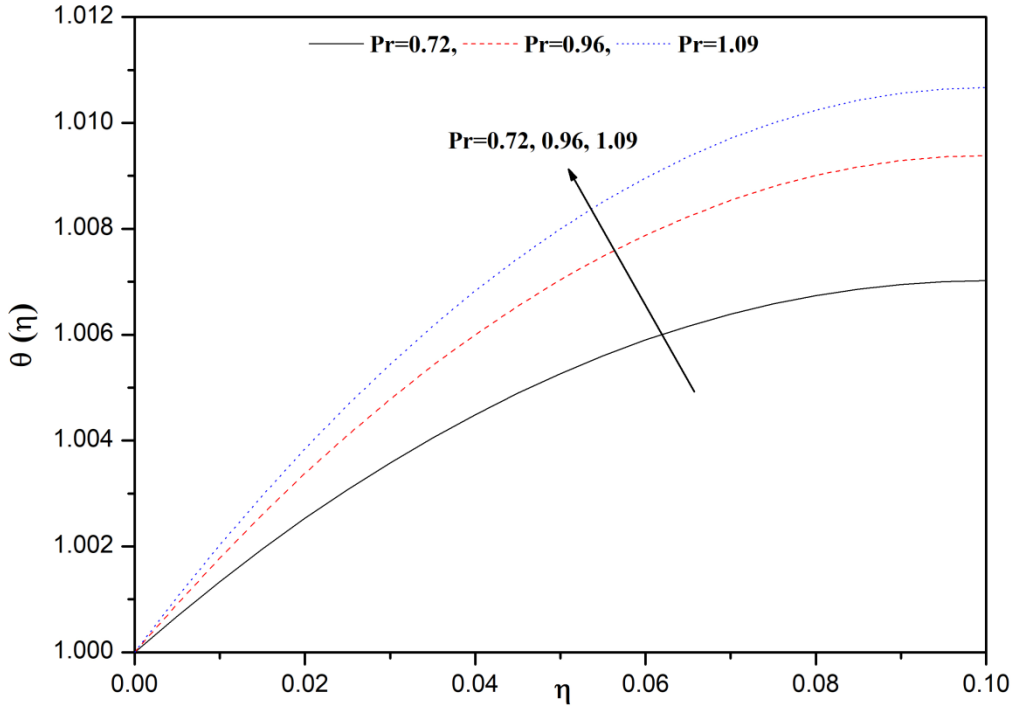

Fig. 6. Temperature profile for difference values of Pr with S= δ=A=Rd=α=0.1, β =10, Mn=0.5

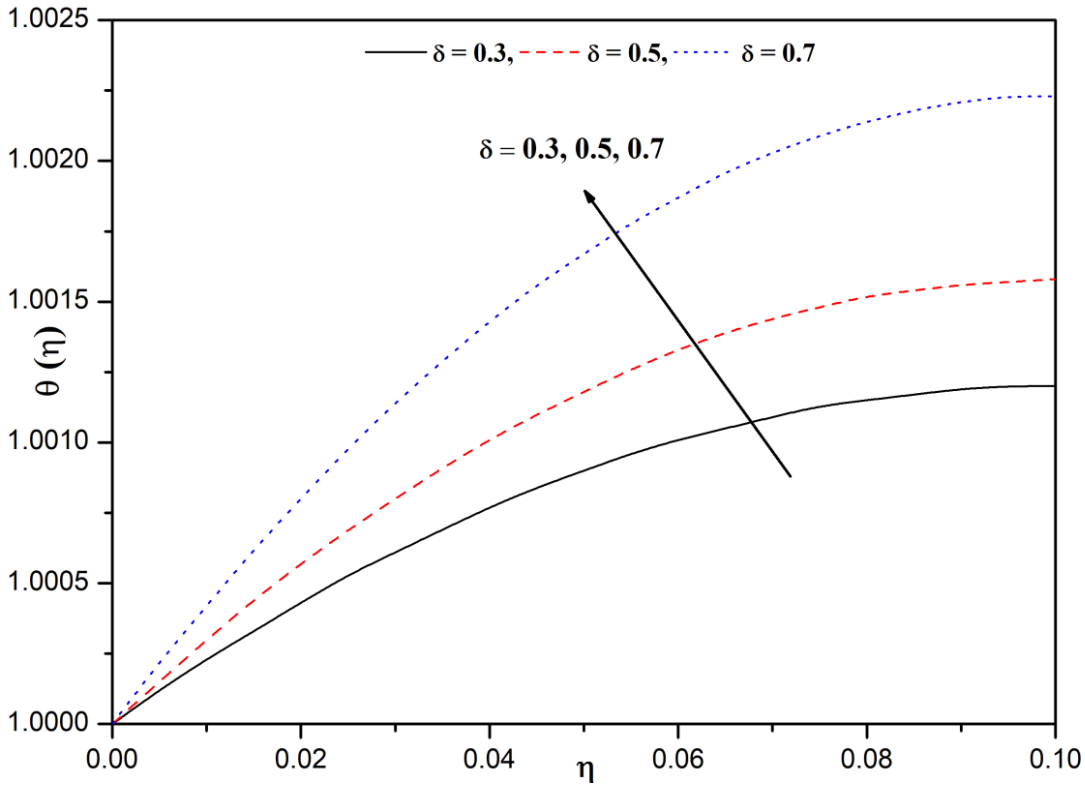

Fig. 7. Temperature profile for difference values of δ with Pr=0.72, S= A=Rd=α=0.1, β =10, Mn=0.5

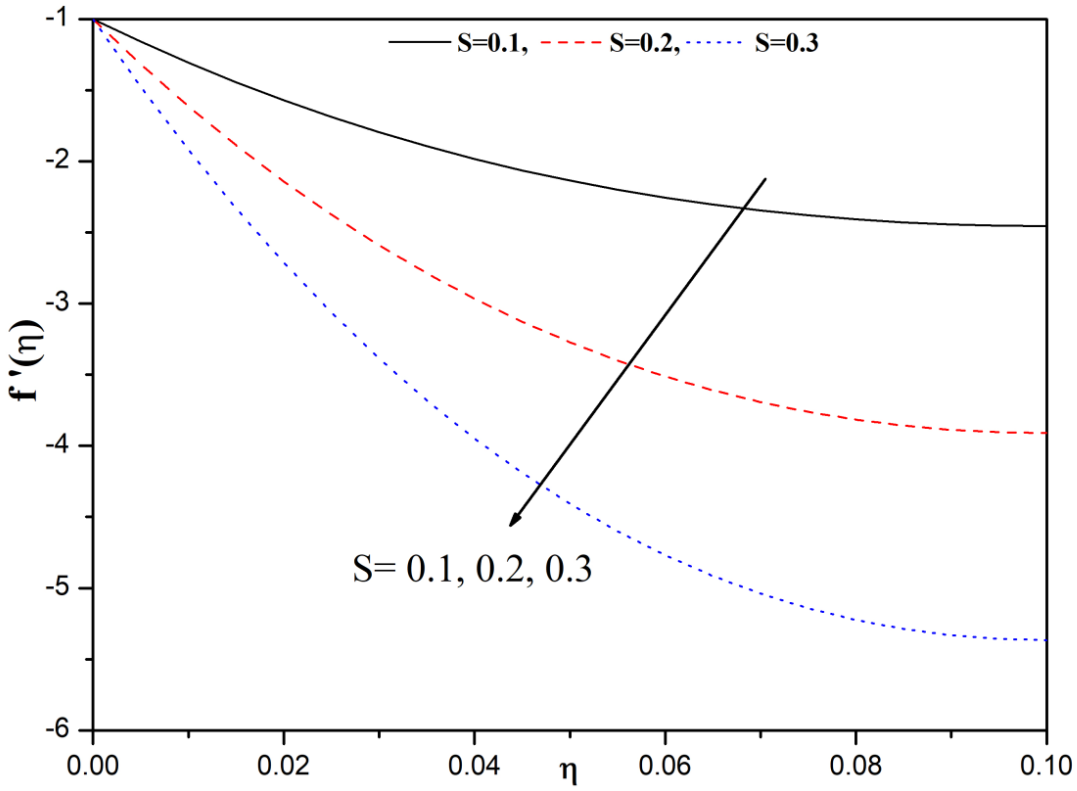

Fig. 8. Velocity profile for difference values of S with Pr=0.72, A=δ=Rd=α=0.1, β =10, Mn=0.5

Table 2
The values of skin friction coefficient and Nusselt number for different physical parameters

β	A	Mn	Rd	Pr	δ	S	$f''(0)$	$\theta'(0)$
1							0.00508	0.01937
2	0.1						0.00496	0.01937
10		0.5					0.00487	0.01937
	0.1						0.00487	0.01937
	0.5		0.1				0.00476	0.01937
	1			0.72			0.00463	0.01937
		0.1			0.1		0.00878	0.01937
		0.3					0.00682	0.01937
		0.5				0.1	0.00487	0.01937
			0.1				0.00487	0.01937
			0.3				0.00487	0.01539
10			0.5				0.00487	0.01277
				0.72			0.00487	0.14033
	0.1			0.96			0.00487	0.18722
		0.5		1.09			0.00487	0.21321
					0.3		0.00487	0.02402
			0.1		0.5		0.00487	0.03156
				0.72	0.7		0.00487	0.04464
						0.1	0.00487	0.01937
					0.1	0.2	0.00392	0.01937
						0.3	0.00284	0.01937

Table 2 presents the numerical values of skin friction and Nusselt number ($f''(0)$ *and* $\theta'(0)$)for various values of embedding parameters. It is evident that the impact of the Casson parameter, Hartman number, variable viscosity parameter, and steadiness parameter decreases skin friction. On the other hand, the Prandtl number and Thermal conductivity parameter increase the Nusselt number, while a reverse trend is observed in the case of the Radiation parameter.

5. Conclusions

In conclusion, our study has highlighted several key findings regarding the effects of various parameters on the flow and heat transfer characteristics of Casson fluids in magnetohydrodynamic (MHD) boundary layer flows over a stretching sheet.

i. The Casson parameter and Hartman number exhibit an opposing effect on fluid momentum.
ii. The variable viscosity parameter leads to a reduction in the velocity profile, and a similar trend is observed in the case of the steadiness parameter S.
iii. The influence of the Radiation parameter and Prandtl number on fluid temperature shows a contrasting behaviour.
iv. The thermal conductivity parameter has a positive effect, enhancing the temperature of the fluid.

Further investigation could focus on finding the optimal combination of the Casson parameter and Hartman number to achieve specific flow characteristics or heat transfer rates. Also, future research could explore the contrasting behaviour of the Radiation Parameter and Prandtl Number on fluid temperature to develop more accurate models for predicting heat transfer in MHD flow systems.

Acknowledgement
This research was not funded by any grant.

References
[1] Casson, N. "Flow equation for pigment-oil suspensions of the printing ink-type." *Rheology of disperse systems* (1959): 84-104.
[2] Fredrickson, Arnold Gerhard. "Principles and applications of rheology." (1964): 13.
[3] Attia, Hazem A. "Unsteady hydromagnetic channel flow of dusty fluid with temperature dependent viscosity and thermal conductivity." *Heat and mass transfer* 42, no. 9 (2006): 779-787. https://doi.org/10.1007/s00231-005-0044-z
[4] Mitsoulis, E. "Flows of Viscoelastic Materials: Models and Computations." In *The British Society of Rheology*, 135–178. 2007.
[5] Kameswaran, P. K., M. Narayana, P. Sibanda, and P. V. S. N. Murthy. "Hydromagnetic nanofluid flow due to a stretching or shrinking sheet with viscous dissipation and chemical reaction effects." *International Journal of Heat and Mass Transfer* 55, no. 25-26 (2012): 7587-7595. https://doi.org/10.1016/j.ijheatmasstransfer.2012.07.065
[6] Hayat, T., S. A. Shehzad, and A. Alsaedi. "Soret and Dufour effects on magnetohydrodynamic (MHD) flow of Casson fluid." *Applied Mathematics and Mechanics* 33 (2012): 1301-1312. https://doi.org/10.1007/s10483-012-1623-6
[7] Umavathi, Jawali C., A. J. Chamkha, and Syed Mohiuddin. "Combined effect of variable viscosity and thermal conductivity on free convection flow of a viscous fluid in a vertical channel." *International Journal of Numerical Methods for Heat & Fluid Flow* 26, no. 1 (2016): 18-39. https://doi.org/10.1108/HFF-12-2014-0385
[8] Yazdi, M. H., S. Abdullah, I. Hashim, and K. Sopian. "Slip MHD liquid flow and heat transfer over non-linear permeable stretching surface with chemical reaction." *International Journal of Heat and Mass Transfer* 54, no. 15-16 (2011): 3214-3225. https://doi.org/10.1016/j.ijheatmasstransfer.2011.04.009

[9] Bhattacharyya, Krishnendu, and G. C. Layek. "Slip effect on diffusion of chemically reactive species in boundary layer flow over a vertical stretching sheet with suction or blowing." *Chemical Engineering Communications* 198, no. 11 (2011): 1354-1365. https://doi.org/10.1080/00986445.2011.560515

[10] Khan, Yasir, Qingbiao Wu, Naeem Faraz, and Ahmet Yildirim. "The effects of variable viscosity and thermal conductivity on a thin film flow over a shrinking/stretching sheet." *Computers & Mathematics with Applications* 61, no. 11 (2011): 3391-3399. https://doi.org/10.1016/j.camwa.2011.04.053

[11] Mukhopadhyay, Swati. "Casson fluid flow and heat transfer over a nonlinearly stretching surface." *Chinese Physics B* 22, no. 7 (2013): 074701. https://doi.org/10.1088/1674-1056/22/7/074701

[12] Afify, Ahmed A. "The influence of slip boundary condition on Casson nanofluid flow over a stretching sheet in the presence of viscous dissipation and chemical reaction." *Mathematical Problems in Engineering* 2017, no. 1 (2017): 3804751. https://doi.org/10.1155/2017/3804751

[13] Aurangzaib, A. R. M. Kasim, N. F. Mohammad, and Sharidan Shafie. "Effect of thermal stratification on MHD free convection with heat and mass transfer over an unsteady stretching surface with heat source, Hall current and chemical reaction." *International Journal of Advances in Engineering Sciences and Applied Mathematics* 4 (2012): 217-225. https://doi.org/10.1007/s12572-012-0066-y

[14] Shehzad, S. A., T. Hayat, M. Qasim, and S. Asghar. "Effects of mass transfer on MHD flow of Casson fluid with chemical reaction and suction." *Brazilian journal of chemical engineering* 30 (2013): 187-195. https://doi.org/10.1590/S0104-66322013000100020

[15] Pal, Dulal, and Gopinath Mandal. "Influence of thermal radiation on mixed convection heat and mass transfer stagnation-point flow in nanofluids over stretching/shrinking sheet in a porous medium with chemical reaction." *Nuclear Engineering and Design* 273 (2014): 644-652. https://doi.org/10.1016/j.nucengdes.2014.01.032

[16] Gireesha, Bijjanal Jayanna, M. R. Krishnamurthy, Ballajja Chandrappa Prasannakumara, and Rama Subba Reddy Gorla. "MHD flow and nonlinear radiative heat transfer of a Casson nanofluid past a nonlinearly stretching sheet in the presence of chemical reaction." *Nanoscience and Technology: An International Journal* 9, no. 3 (2018). https://doi.org/10.1615/NanoSciTechnolIntJ.2018020102

[17] Khan, Arshad, Dolat Khan, Ilyas Khan, Farhad Ali, and Muhammad Imran. "MHD flow of sodium alginate-based Casson type nanofluid passing through a porous medium with Newtonian heating." *Scientific reports* 8, no. 1 (2018): 1-12. https://doi.org/10.1038/s41598-018-26994-1

[18] Ibrahim, S. M., P. V. Kumar, G. Lorenzini, E. Lorenzini, and F. Mabood. "Numerical study of the onset of chemical reaction and heat source on dissipative MHD stagnation point flow of Casson nanofluid over a nonlinear stretching sheet with velocity slip and convective boundary conditions." *Journal of engineering thermophysics* 26 (2017): 256-271. https://doi.org/10.1134/S1810232817020096

[19] Animasaun, I. L. "Effects of thermophoresis, variable viscosity and thermal conductivity on free convective heat and mass transfer of non-darcian MHD dissipative Casson fluid flow with suction and nth order of chemical reaction." *Journal of the Nigerian Mathematical Society* 34, no. 1 (2015): 11-31.

[20] Damseh, Rebhi A., M. Q. Al-Odat, Ali J. Chamkha, and Benbella A. Shannak. "Combined effect of heat generation or absorption and first-order chemical reaction on micropolar fluid flows over a uniformly stretched permeable surface." *International Journal of Thermal Sciences* 48, no. 8 (2009): 1658-1663. https://doi.org/10.1016/j.ijthermalsci.2008.12.018

[21] Magyari, Eugen, and Ali J. Chamkha. "Combined effect of heat generation or absorption and first-order chemical reaction on micropolar fluid flows over a uniformly stretched permeable surface: The full analytical solution." *International Journal of Thermal Sciences* 49, no. 9 (2010): 1821-1828. https://doi.org/10.1016/j.ijthermalsci.2010.04.007

[22] Malik, M. Y., M. Naseer, S. Nadeem, and Abdul Rehman. "The boundary layer flow of Casson nanofluid over a vertical exponentially stretching cylinder." *Applied Nanoscience* 4 (2014): 869-873. https://doi.org/10.1007/s13204-013-0267-0

[23] Pramanik, S. "Casson fluid flow and heat transfer past an exponentially porous stretching surface in presence of thermal radiation." *Ain shams engineering journal* 5, no. 1 (2014): 205-212. https://doi.org/10.1016/j.asej.2013.05.003

[24] Siddiqui, Abdul M., Sania Irum, and Ali R. Ansari. "Unsteady squeezing flow of a viscous MHD fluid between parallel plates, a solution using the homotopy perturbation method." *Mathematical Modelling and Analysis* 13, no. 4 (2008): 565-576. https://doi.org/10.3846/1392-6292.2008.13.565-576

[25] Prasad, K. V., K. Vajravelu, Hanumesh Vaidya, and Robert A. Van Gorder. "MHD flow and heat transfer in a nanofluid over a slender elastic sheet with variable thickness." *Results in physics* 7 (2017): 1462-1474. https://doi.org/10.1016/j.rinp.2017.03.022

[26] Prasad, K. V., Hanumesh Vaidya, Oluwole Daniel Makinde, and B. Srikantha Setty. "MHD mixed convective flow of Casson nanofluid over a slender rotating disk with source/sink and partial slip effects." In *Defect and diffusion*

forum, vol. 392, pp. 92-122. Trans Tech Publications Ltd, 2019. https://doi.org/10.4028/www.scientific.net/DDF.392.92

[27] Vaidya, Hanumesh, and Kerehalli Vinayaka Prasad. "Significances of homogeneous-heterogeneous reactions on casson fluid over a slippery stretchable rotating disk with variable thickness." *CFD Letters* 11, no. 4 (2019): 41-63.

[28] Vaidya, Hanumesh, K. V. Prasad, Kuppalapalle Vajravelu, B. Srikantha Setty, and Oluwole Daniel Makinde. "Influence of variable liquid properties on magnetohydrodynamic flow and heat transfer of a Casson liquid over a slender rotating disk: numerical and optimal solution." *Computational Thermal Sciences: An International Journal* 12, no. 1 (2020). https://doi.org/10.1615/ComputThermalScien.2019029098

[29] Ramanuja, Mani, G. Gopi Krishna, Hari Kamala Sree, and S. R. Mishra. "Characteristics of Newtonian heating on electrically conducting water-based nano-fluid with in permeable vertical micro-channels." *J. Math. Comput. Sci.* 12 (2021): Article-ID.

[30] Ramanuja, M., J. Kavitha, A. Sudhakar, and N. Radhika. "Study of MHD SWCNT-Blood Nanofluid Flow in Presence of Viscous Dissipation and Radiation Effects through Porous Medium." *Journal of the Nigerian Society of Physical Sciences* (2023): 1054-1054. https://doi.org/10.46481/jnsps.2023.1054

[31] Reddy, Y. Dharmendar, V. Srinivasa Rao, and M. Anil Kumar. "Effect of heat generation/absorption on MHD copper-water nanofluid flow over a non-linear stretching/shrinking sheet." In *AIP Conference Proceedings*, vol. 2246, no. 1. AIP Publishing, 2020. https://doi.org/10.1063/5.0014438

[32] Goud, B. Shankar, Yanala Dharmendar Reddy, Nawal A. Alshehri, Wasim Jamshed, Rabia Safdar, Mohamed R. Eid, and Mohamed Lamjed Bouazizi. "Numerical case study of chemical reaction impact on MHD micropolar fluid flow past over a vertical riga plate." *Materials* 15, no. 12 (2022): 4060. https://doi.org/10.3390/ma15124060

[33] Bejawada, Shankar Goud, Wasim Jamshed, Rabia Safdar, Yanala Dharmendar Reddy, Meznah M. Alanazi, Heba Y. Zahran, and Mohamed R. Eid. "Chemical reactive and viscous dissipative flow of magneto nanofluid via natural convection by employing Galerkin finite element technique." *Coatings* 12, no. 2 (2022): 151. https://doi.org/10.3390/coatings12020151

[34] Sridhar, Wuriti, Talla Hymavathi, Sameh E. Ahmed, Abdulaziz Alenazi, and Ganugapati Raghavendra Ganesh. "Keller Box procedure for stagnation point flow of EMHD Casson nanofluid over an absorbent stretched electromagnetic plate with chemical reaction." *Numerical Heat Transfer, Part A: Applications* 85, no. 17 (2024): 2851-2868. https://doi.org/10.1080/10407782.2023.2229949

[35] Shankar Goud, Bejawada, Yanala Dharmendar Reddy, and Satyaranjan Mishra. "Joule heating and thermal radiation impact on MHD boundary layer Nanofluid flow along an exponentially stretching surface with thermal stratified medium." *Proceedings of the Institution of Mechanical Engineers, Part N: Journal of Nanomaterials, Nanoengineering and Nanosystems* 237, no. 3-4 (2023): 107-119. https://doi.org/10.1177/23977914221100961

[36] Mahmood, Zafar, Saad Althobaiti, Adnan, and Umar Khan. "Nanoparticle aggregation effect over MHD oblique stagnation point flow of the convective surface of nanoliquids." *Proceedings of the Institution of Mechanical Engineers, Part N: Journal of Nanomaterials, Nanoengineering and Nanosystems* (2023): 23977914231214863. https://doi.org/10.1177/23977914231214863

[37] Rafique, Khadija, Zafar Mahmood, Aisha M. Alqahtani, Awatif MA Elsiddieg, Umar Khan, Wejdan Deebani, and Meshal Shutaywi. "Impacts of thermal radiation with nanoparticle aggregation and variable viscosity on unsteady bidirectional rotating stagnation point flow of nanofluid." *Materials Today Communications* 36 (2023): 106735. https://doi.org/10.1016/j.mtcomm.2023.106735

[38] Adnan, Raad Suhail Ahmed, Iman Adnan Annon, Sundus M. Noori, and Dauod Selman Dauod. "Effect of short heat treatment on mechanical properties and shape memory properties of Cu–Al–Ni shape memory alloy." *Open Engineering* 14, no. 1 (2024): 20240013. https://doi.org/10.1515/eng-2024-0013

[39] Ali, Bilal, Sidra Jubair, Zafar Mahmood*, and Md Irfanul Haque Siddiqui. "Electrically conducting mixed convective nanofluid flow past a nonlinearly slender Riga plate subjected to viscous dissipation and activation energy." *Modern Physics Letters B* (2024): 2450336. https://doi.org/10.1142/S0217984924503366

[40] Rafique, Khadija, Zafar Mahmood, Adnan, Umar Khan, Taseer Muhammad, Magda Abd El-Rahman, Sanaa A. Bajri, and Hamiden Abd El-Wahed Khalifa. "Numerical investigation of entropy generation of Joule heating in non-axisymmetric flow of hybrid nanofluid towards stretching surface." *Journal of Computational Design and Engineering* 11, no. 2 (2024): 146-160. https://doi.org/10.1093/jcde/qwae029

[41] Brewster, M. Quinn. *Thermal radiative transfer and properties*. John Wiley & Sons, 1992.

[42] Liao, Shijun. "An optimal homotopy-analysis approach for strongly nonlinear differential equations." *Communications in Nonlinear Science and Numerical Simulation* 15, no. 8 (2010): 2003-2016. https://doi.org/10.1016/j.cnsns.2009.09.002